

Height Fluctuations and Intermittency of V_2O_5 Films by Atomic Force Microscopy

A. Irajizad ^a, G. Kavei ^b, M. Reza Rahimi Tabar ^{a,c,d},
and S.M. Vaez Allaei ^e

^a *Dept. of Physics, Sharif University of Technology, P.O.Box 11365-9161, Tehran, Iran*

^b *Material and Energy, Research Center, P. O. Box 14155-4777, Tehran, Iran*

^c *CNRS UMR 6529, Observatoire de la Côte d'Azur, BP 4229, 06304 Nice Cedex 4, France*

^d *Dept. of Physics, Iran University of Science and Technology, Narmak, Tehran 16844, Iran*

^e *Institute for Advanced Studies in Basic Sciences, P. O. Box 45195-159, Zanjan, Iran*

The spatial scaling law and intermittency of the V_2O_5 surface roughness by atomic force microscopy has been investigated. The intermittency of the height fluctuations has been checked by two different methods, first, by measuring scaling exponent of q -th moment of height-difference fluctuations i.e. $C_q = \langle |h(x_1) - h(x_2)|^q \rangle$ and the second, by defining generating function $Z(q, N)$ and generalized multi-fractal dimension D_q . These methods predict that there is no intermittency in the height fluctuations. The observed roughness and dynamical exponents can be explained by the numerical simulation on the basis of forced Kuramoto-Sivashinsky equation.

PACS: 52.75.Rx, 68.35.Ct.

I. INTRODUCTION

Due to the technical importance and fundamental interest, a great deal of effort has been devoted to understanding the mechanism of thin-film growth and the kinetic roughening of growing surfaces in various growth techniques. Analytical and numerical treatments of simple growth models suggest, quite generally, the height fluctuations have a self-similar character and their average correlations exhibit a dynamic scaling form [1-6].

Vanadium pentoxide, V_2O_5 , has been the subject of intense work because of its diverse applications in catalytic oxidation reactions, cathodic electrode in solid state micro-batteries, windows and electrochromic devices as well as gas sensors and to be of interest for transmittance modulation in smart windows with potential application in the architecture and automotive. Also V_2O_5 is a low mobility semiconductor, and having predominantly an n-type. Electrons are the charge carriers, and an increase in the carrier density in accompanied by reduction in oxygen concentration in the lattice [7-9].

This work aims to study the roughness and dynamical exponents (χ and z) and the intermittency of the V_2O_5 films by the atomic force microscopy. We measure the height-difference moments $C_q(l = |x_1 - x_2|) = \langle |h(x_1) - h(x_2)|^q \rangle$ and show that they behave as $\sim |x_1 - x_2|^{\xi_q}$. The obtained ξ_q is a linear function of q . We also introduce the generating function $Z(q, N)$ and generalized multifractal dimension D_q and show that D_q behave also as a linear function of q . These observations indicate that the height fluctuations are not intermittent. It is also argued that the measured roughness and dynamical exponents belong to early-time scaling regime of the noisy Kuramoto-Sivashinsky equation.

II. EXPERIMENTS

V_2O_5 layers were grown on the polished Si(100) substrate by resistive evaporation method in a high vacuum chamber. The pressure during evaporation was 10^{-5} torr. The thickness of the growing films was measured in situ by a quartz crystal thickness monitor. We performed all deposition at room temperature, with deposition rate about $10 - 15 \text{ nm/min}$. However, during the film deposition the substrate temperature raised to $T \sim 60C^0$, due to the radiation effect of alumina boat. The substrate temperature was determined using chromel/alumel thermocouple mounted in close proximity of samples. Surface composition of samples was measured by Auger electron spectroscopy (AES) using a 3 keV electron beam and a cylindrical mirror analyzer (Varian model 981-2607). The surface topography of the films was investigated using Park Scientific Instruments model Autoprobe CP. The images are collected in a constant force mode and digitized into 256×256 pixels with scanning frequency of 0.6 Hz. The cantilever of 0.05 N m^{-1} spring constant with a commercial standard pyramidal Si_3N_4 tips has been used. A variety of scans, each with size L were recorded at random locations on the V_2O_5 film surface. In order to determine the structure of the deposited V_2O_5 films, we have performed XRD measurements of samples. The spectra for the as-deposited V_2O_5 films grown showed that the V_2O_5 thin films are amorphous. For thick films ($d > 200 \text{ nm}$) two very broad weak peaks were observed representing the growth of (001) and (002) peaks of the V_2O_5 orthorhombic structure[7]. The yellow color of deposited oxide films and their optical transmission spectra indicates the existence of V_2O_5 structure rather than other vanadium oxide phases[8]. AES analysis of the V_2O_5 samples showed V and O peaks at the surface of the deposited films. The stoichiometry of the vanadium oxide films was calculated from the ratio of O

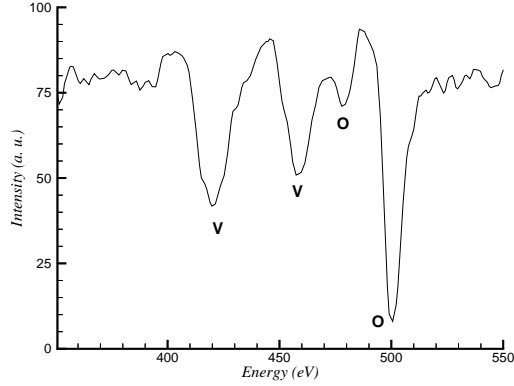


FIG. 1. AES spectra from V_2O_5 surface. The O/V ratio is 2.5 ± 0.1 (by considering the elemental sensitivity factors).

to V Auger peak heights by considering the elemental sensitivity factors. The O/V ratio was 2.5 ± 0.1 indicating the formation of stoichiometric vanadium pentoxide at the surface of the thin film (see Fig.1). With these observations we conclude the film composition is nearly stiochiometric[9].

III. RESULTS

Figure 2 shows the variation of the surface morphology for different growth times (or thickness) of processed samples by AFM. As deposition proceeds, the size of mountains and valleys grows until the system approaches to a stationary state in which the thickness is about $150nm$.

The quantitative information of the surface morphology can be derived by considering a sample of size L , and defining the mean height of growing film \bar{h} and, its roughness w through [10]:

$$\bar{h}(L, t) = \frac{1}{L} \int_{-L/2}^{L/2} dx h(x, t) \quad (1)$$

and

$$w(L, t) = (\langle (h - \bar{h})^2 \rangle)^{1/2}. \quad (2)$$

$\langle \dots \rangle$ denotes an averaging over different realization (samples). Starting from a flat interface (one of the possible initial conditions), it was conjectured by Family and Vicsek [11] that a scaling of space by factor b and of time by a factor b^z (z is the dynamical scaling exponent), re-scales the roughness w by factor b^x as follows: $w(bL, b^z t) = b^x w(L, t)$, which implies that

$$w(L, t) = L^x f(t/L^z). \quad (3)$$

If for large t and fixed L ($t/L^z \rightarrow \infty$), w saturates then $f(x) \rightarrow const.$, as $x \rightarrow \infty$. However, for a fixed large

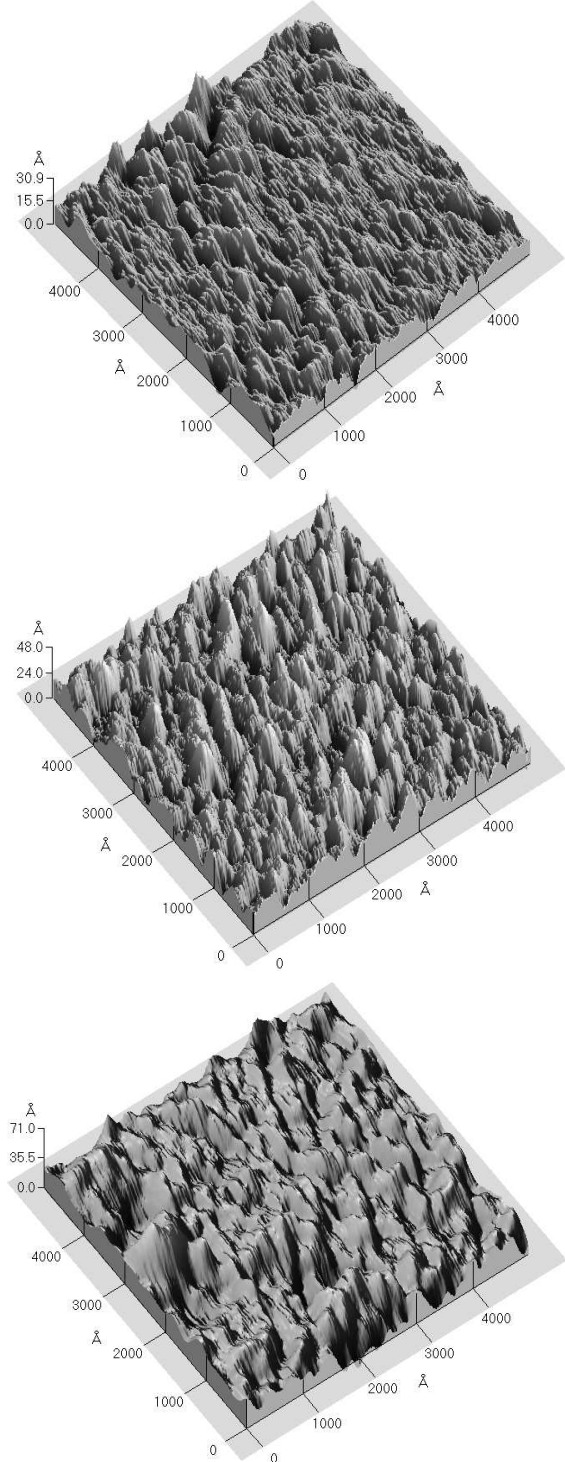


FIG. 2. AFM surface images (all $0.5 \times 0.5 \mu m^2$) of V_2O_5 films with thickness of (a) 20nm , (b)100nm, (c) 260 nm. (from up to down)

L and $1 \ll t \ll L^z$, one expects that correlations of the height fluctuations are set up only within a distance $t^{1/z}$ and thus must be independent of L . This implies that for $x \ll 1$, $f(x) \sim x^\beta$ with $\beta = \chi/z$. Thus dynamic scaling postulates that, $w(L, t) \sim t^\beta$ for $1 \ll t \ll L^z$ and $\sim L^\chi$ for $t \gg L^z$. The roughness exponent χ and the dynamic exponent z characterize the self-affine geometry of the surface and its dynamics, respectively. We measure the exponent χ from equal-time height-height correlation function defined as $C_2(l = |x_1 - x_2|) = \langle |h(x_1) - h(x_2)|^2 \rangle$. Here $h(\mathbf{x})$ is the surface height at position \mathbf{x} on the surface relative to the mean surface height.

In order to determine the roughness exponent $\chi = \xi_2/2$, we consider the roughness of the samples with thickness $20nm$, $100nm$ and $260nm$. Fig.3 shows that, for the thickness $20nm$ and $100nm$, the scaling behavior exists only for the scaling region $\sim 4nm$ to $20nm$, but for the stationary state sample, $\langle h \rangle = 260nm$, there is a cross over for the scaling exponent $\chi = \xi_2/2$ in $l = l^* \approx 22nm$. The exponent is ξ_{21} for the length scales $4nm$ to the scale l^* , and for the length scales $25nm \leq l \leq 50nm$, the fluctuation is determined by another exponent ξ_{22} . The measured values for the exponents ξ_{21} and ξ_{22} are 1.64 ± 0.06 ($\chi_1 = 0.83 \pm 0.03$) and 0.58 ± 0.08 ($\chi_2 = 0.29 \pm 0.04$) respectively. The measured roughness exponent χ of the samples $20nm$, $100nm$ and $150nm$ are 0.71 ± 0.04 , 0.77 ± 0.03 and 0.82 ± 0.03 , respectively. As shown in Figs. 4 and 5, we note that the correlation length l^* is about $22nm$. Therefore, we are dealing with the statistical properties of the correlated scaling surfaces. As discussed in [22], such systems exhibit the sampling-induced hidden cycles (log-periodic fluctuations [23]). Such oscillatory behavior will diminish when the sampling size is sufficiently large. The oscillation amplitude approaches zero to within an order of $\delta = \sqrt{(l^*/ML)}$, where L and M are the sampling size and the number of independent curves which are averaged. We have determined each exponents by averaging on the eight AFM images. In our averaging it appears that there is no log-periodic property for the height-height correlation function. Therefore the surfaces of V_2O_5 are self-affine.

The existence of the cross over scale l^* in the stationary state is not observed only in the second moment C_2 . In Fig.4 log-log plot of C_3 vs l for the three samples are presented. It is evident that for the stationary state sample, the scaling exponent of the third moment C_3 has also a cross over in l^* . The measurement shows that in the stationary state the exponents ξ_{3i} behave as $\xi_{3i} = 3/2\xi_{2i}$ with $i = 1, 2$.

We also examine the scaling behaviour of the q -th moment of the height-difference $C_q = \langle |h(x_1) - h(x_2)|^q \rangle$ and show that all of the moments at least up to $q = 20$ behave as $|x_1 - x_2|^{\xi_q}$. Fig.5 shows ξ_q vs q for $260nm$ sample in $25nm \leq l \leq 50nm$ scaling region. The graph

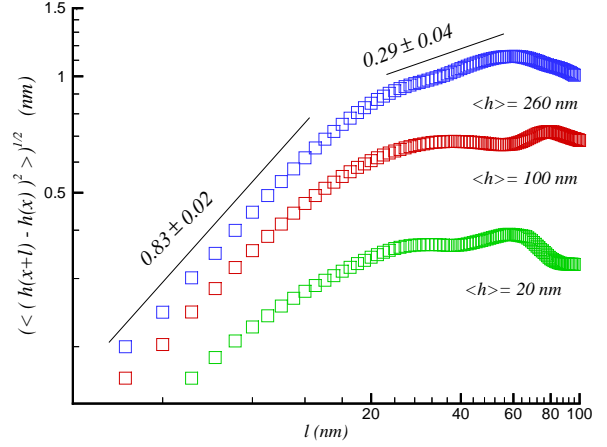


FIG. 3. Log-log plot of the second moment of height-difference vs l , which shows that for samples with thickness $20nm$ and $100nm$ the scaling region is $4nm < l < 20nm$ and for the sample with thickness $260nm$ there is a cross over scale $l^* \approx 22nm$. The upper and lower parts of height-height correlation function have the roughness exponent 0.29 ± 0.04 and 0.83 ± 0.03 , respectively.

of ξ_q for the $4nm \leq l \leq 20nm$ region is the same as Fig.5 but with different slope. In the two scaling regions, the ξ_q 's have a linear dependence on q . This measurement indicates that the height-fluctuations are not intermittent and all of scaling exponents in the stationary state can be expressed by ξ_{2i} , $i = 1, 2$ only.

There is another method to check that the intermittency is absent in the height fluctuations of V_2O_5 surface [12-13]. Let's introduce the generating function $Z(q, N; l)$. The generating function is defined through

$$Z(q, N; l) = \sum_{i=1}^N \mu_i^q, \quad (4)$$

where the normalized measure $\mu_i \geq 0$ is

$$\mu_i = \frac{|h(x_i + l) - h(x_i)|}{\sum_{i=1}^N |h(x_i + l) - h(x_i)|}, \quad (5)$$

and, N is the number of data $|h(x_i + l) - h(x_i)|$. For large N , the generating function Z scales as $Z(q, N; l) \sim N^{-\tau(q)}$. We measure the exponent $\tau(q) = (q - 1)D_q$ in both scaling region ($4nm$ to $20nm$ and $25nm$ to $50nm$). The amplitude of Z depends only on l and q . In Fig.6 we plot the $(1 - q)D_q$ vs q for small l . The figure shows that the $\tau(q)$ has a linear dependence on q and the generalized fractal dimension D_q is independent of q . Its value is $D_q = D_0 = 7.34 \pm 0.02$. Therefore we conclude that the height fluctuation is not intermittent. It is necessary to note that the exponents ξ_q and D_q are not independent in the small region of l . Defining $\xi_q = qH_q$, it has been

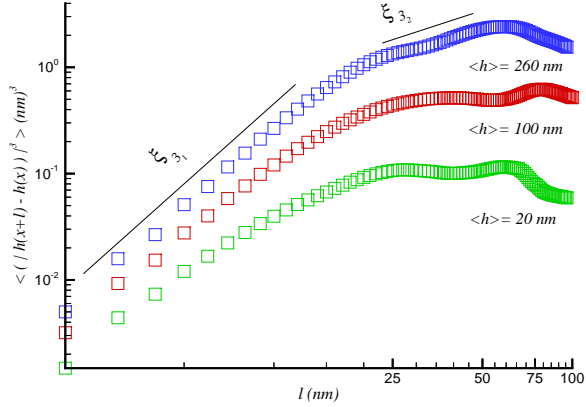


FIG. 4. log-log plot of the third moment of height-difference vs l , which shows that in the length scale $l^* \approx 22 \text{ nm}$ there is also a cross over for the scaling exponent ξ_3 of the sample 260 nm .

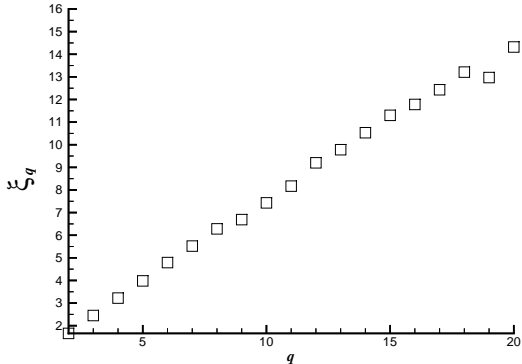


FIG. 5. The plot of ξ_q vs q , which has a linear dependence on q and shows that the height-difference fluctuations are not intermittent.

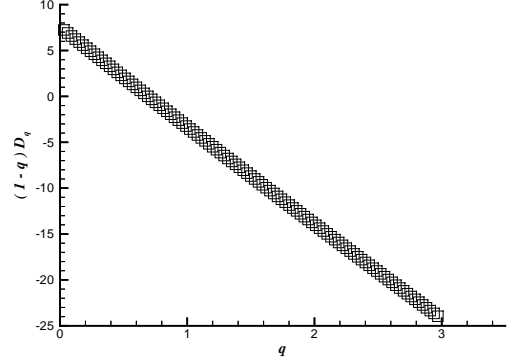


FIG. 6. Plot of $(1-q)D_q$ vs q , shows that the fluctuations are determined only by dimension D_0 and the surface are not intermittent in the scaling region.

shown in [20] that H_q can be expressed in terms of D_q as;

$$H_q = H_1 + \frac{(q-1)(D_q - D_{eff})}{q}. \quad (6)$$

Our measurement for H_q shows that the H_q is independent of q and this means that $D_{eff} = D_q = D_0$. Let us discuss the origin of the D_{eff} in eq.(6). To evaluate the C_q we should calculate the summation $\frac{1}{N} \sum_{i=1}^N |h(x_i) - h(x_i + l)|^q$, where N is the number of points over which the average is taken. Normally small l is meant by $l \sim 1/N$. The authors of Ref.[20] assumed that, in evaluation of C_q , l and N may be related in a way different from $l \sim 1/N$. That is $N \sim l^{-D_{eff}}$ (D_{eff} could be considered here as a fractal dimension of the effective support of the process). The choice of a particular partition has no effect on the H_q spectrum. However, D_{eff} enters the relation between H_q and generalized dimension D_q as expressed in eq.(6).

IV. DISCUSSION AND GROWTH MODEL

In our experiments we obtain a region in which the growth exponents of V_2O_5 are consistent with early-scaling regime of forced Kuramoto-Sivashinsky (KS) equation in 2+1 dimensions [19]. The forced Kuramoto-Sivashinsky has the following form [14-19],

$$\frac{\partial h}{\partial t} = \nu \nabla^2 h - k \nabla^4 h + (\lambda/2)(\nabla h)^2 + \eta(x, t) \quad (7)$$

where the ν, k and λ are the surface tension, surface diffusion and non-linear factor, respectively. The force η is a noise term reflecting spatial and temporal fluctuation in the incoming flux of material and has a Gaussian distribution and uncorrelated in space and time. In the limit $k = 0$ and for $\nu > 0$ the forced KS equation reduces to

the Kardar-Parisi-Zhang (KPZ) equation. The KS equation with $\lambda = 0$ is a linear equation and can be exactly solved by the standard methods [19,22]. For some Gaussian noise term, because of the linearity the probability distribution function (PDF) of $h - \bar{h}$ is also Gaussian. It is discussed in [22] that for $\lambda = 0$ and $\nu/k < 0$ the KS equation generates a mound surface and for $\nu/k > 0$ gives a self-affine surface, with a roughness exponent $\simeq 1$. For $\lambda \neq 0$ the nonlinear term breaks the symmetry under transformation $h \rightarrow -h$. Therefore the PDF of $h - \bar{h}$ must be skewed. Our measured value for the PDF of $h - \bar{h}$ shows that the PDF has positive skewness. We will report the skewness and kurtosis of the PDF of the V_2O_5 films elsewhere [12].

Recent simulation of KS equation reveals the presence of the early and long scaling regimes [19]. The initial-time values for the growth exponent β and the roughness exponent χ are found to be $0.22 - 0.25$ and $0.75 - 0.80$ respectively. The long time scaling regime is determined by the exponents $\beta = 0.16 - 0.21$ and $\chi = 0.25 - 0.28$. The scaling exponents are notably less than the exponents of KPZ equation [19]. The long-time behavior of the KS-equation has an interesting feature. For long-times the height-height correlation function exhibits a bifractal structure with two different roughness exponents (see Fig.11 in ref. [19]). For $\lambda = 2.0$, $\nu = -0.2$ and $k = 2.0$, the upper and lower parts of height-height correlation function have the roughness exponent 0.27 and 0.71 , respectively.

Now let us compare our results with the numerical simulation of KS equation. Using the numerical results of ref.[19] in table II, one can observe that for early-scaling regime of the Kuramoto-Sivashinsky equation the exponents χ and z satisfy the exponent-identity $\chi + z \simeq 4$. Using the time dependence of roughness of the samples with thickness $20nm$, $50nm$, $100nm$, $120nm$ and $150nm$ we find that $\beta = 0.29 \pm 0.04$ (see Fig.7) and therefore $\chi + z = 3.7 \pm 0.4$, which satisfies the exponent-identity within the experimental errors. We also observe the similar bifractal structure of the height-height correlation function in our samples with thickness $260nm$ (see Fig.11 in [19]). To relate the cross over scale l^* to the the surface morphology, we have measured average distance of nearest local maxima \bar{d}_{max} , and obtain that the \bar{d}_{max} is in the same order of magnitude of l^* . This means that, in the stationary state, in average, if the distance between the points x_1 and x_2 lies between the two local maxima of $h(x)$, the dynamics is determined by the roughness exponent χ_1 . Also for the points that the relative distance lies between the next neighbor maximums ($\sim 20 - 40nm$), the dynamics is given by another exponent χ_2 which is less than the KPZ roughness exponent. Our measurements show that the roughness exponent $\chi_2 = 0.29 \pm 0.04$ is less than the the KPZ roughness exponent in $2 + 1$ dimensions i.e. 0.38 .

In summary we have checked the intermittency of

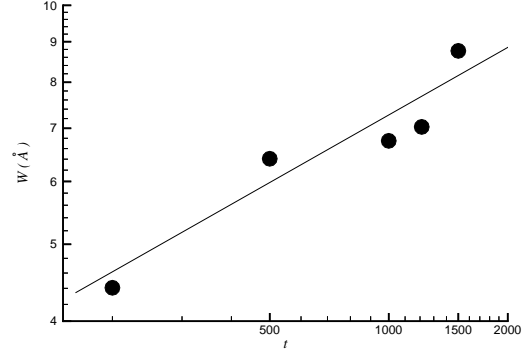


FIG. 7. Log-log plot of the interface width w vs deposition time or thickness (in \AA) t for the samples with thickness $20nm$, $50nm$, $100nm$, $120nm$ and $150nm$. The measured value for β is 0.29 ± 0.04 .

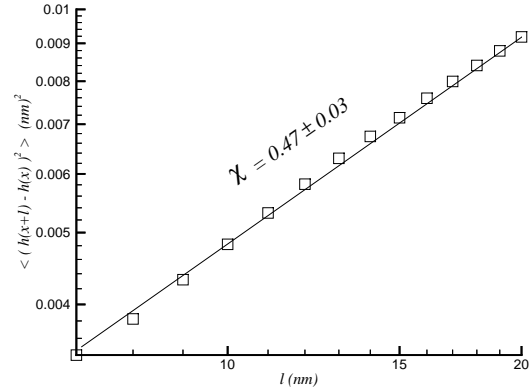


FIG. 8. Log-log plot of the second moment of height-difference vs l , for polished Si(100) substrate. The measured value for the roughness exponent is $\chi_{Si} = 0.47 \pm 0.03$.

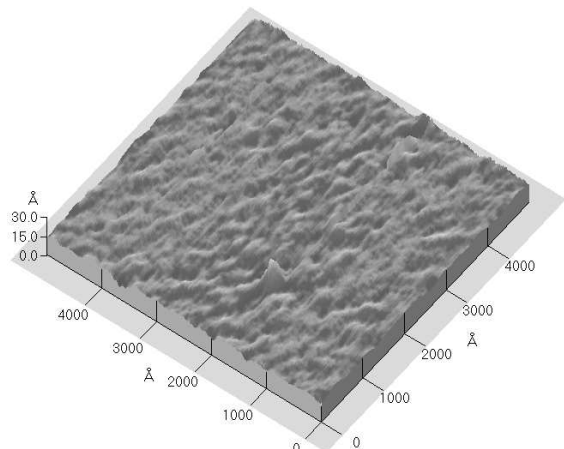


FIG. 9. AFM image of polished Si(100) substrate.

height fluctuation of V_2O_5 via two different methods. These methods predict that the statistics of height fluctuations is not intermittent. We measure the scaling exponents of height-difference moments, $C_q(l = |x_1 - x_2|)$, and show that for small l , they behave as $\sim |x_1 - x_2|^{\xi_q}$. The obtained ξ_q 's are linear function of q . The observation can be explained with the recent numerical simulation on the basis of nonlinear KS equation. However, one should note that for very early stages, when ν term dominates k term, instability arises in x or y direction causing the ripple structure with corresponding wave vector in x or y direction in KS equation. When the ripple structure is formed, there exists slope asymmetry that activates the nonlinear effect. Therefore, in the early-stage of the process, the ripple structure transforms to symmetric mounds. In our experiments we were not able to detect the ripple structure for the samples with $\langle h \rangle \ll 20nm$. It could mean that the polished $Si(100)$ substrate may have an initial roughness which may destroy the ripple structure of the film for very early-stages of the growth. We measure the roughness exponent of the silicon substrate and find that the $\chi_{si} = 0.47 \pm 0.03$ (see Figs.8 and 9).

Finally we note that the measured roughness exponents χ and β can be higher than the true values because of the tip effect [21]. Aue et al. showed that the surface fractal dimension (fractal dimension d_f for 2+1 interface is related to χ by $d_f = 3 - \chi$) determined with a scanning probe technique will always lead to an underestimate of the actual fractal dimension, due to the convolutions of tip and surface. Their analysis included tips with different shapes and aspect ratios. For a tip similar to what we have used, it is suggested that our true χ_1 and χ_2 should be around ~ 0.75 and ~ 0.25 , respectively. We note that the corrected exponents also satisfy the exponent identity.

Acknowledgement

We thank A. Aghamohammadi, F. Azami, M.M. Ahdian, J. Davoudi, A. Farahzadi, G. Ketabi and Z. Vashaei for useful discussions.

- 1998).
- [5] M. Kardar, Physica A **281**,295(2000).
 - [6] A. A. Masoudi, F. Shahbazi, J. Davoudi and M. Reza Rahimi Tabar, Phys. Rev. E **65**, 026132(2002).
 - [7] M. Benmoussa, E. Ibnouelghazi, A. Bennouna and E.L. Ameziane, Thin Solid Films **265**, 22 (1995)
 - [8] S.A. Aly, S.A. Mahmoud, N.Z. El-Sayed and M.A. Kaid, Vacuum **55**,159 (1999)
 - [9] S.N. Svitashva and V.N. Kruchinin, Thin Solid Films **313-314**,319(1998)
 - [10] M. Marsilli, A. Maritan, F. Toigoend J.R. Banavar,Rev. Mod. Phys., **68**,963 (1996)
 - [11] F. Family and T. Vicsek,J.Phys.A **18**,L75(1985)
 - [12] A. Irajizad, G. Kavei, M. Reza Rahimi Tabar and S.M. Vaez Allaei,in preparation.
 - [13] J. Lee and H. E. Stanley, Phys. Rev. Lett. **61**,2945(1988); see also "Fractal and Disordered Systems",Eds. A. Bunde and S. Havlin (Springer-Verlag, p.15,1991).
 - [14] R. M. Bradley, J. M. E. Harper, J. Vac. Sci. Technol. A **6**,2390(1994).
 - [15] R. Cuerno, A.-L. Barabasi, Phys. Rev. Lett. **74**,4746(1995).
 - [16] R. Cuerno, H. A. Makse, S. Tommasone, S. T. Harrington, H. E. Stanley, Phys.Rev.Lett. **75**, 4464(1995).
 - [17] K. B. Lauritsen, R. Cuerno, H. A. Makse, Phys.Rev. E **54**, 3577 (1996).
 - [18] Anthony C.-T. Chan, G.-C. Wang, Surf. Sci. **414**,17-25(1998).
 - [19] J.T. Drotar, Y.-P. Zhao, T.-M. Lu and G.-C. Wang, Phys. Rev. E **59** 177 (1999)
 - [20] A. -L. Barabasi, P. Szepefalusy and T. Vicsed, Physica A **178**, 17 (1991); A. Bershadskii, Phys. Rev. E **58**, 2660 (1998)
 - [21] J. Aue and J. Th. M. De Hosson, Appl. Phys. Lett **71** (10) 1347 (1997)
 - [22] H. -N. Yang, Y. -P. Zhao, A. Chan, T.-M. Lu and G. -C. Wang, Phys. Rev E**56** (1997) 4224
 - [23] N. Abed-pour, A. Aghamohammadi, M. Khorrami and M. Reza Rahimi Tabar, cond-mat/0208544, to appear in Nucl. Phys. B.

-
- [1] A.-L. Barabasi and H. E. Stanley, "Fractal Concepts in Surface Growth" (Cambridge University Press, New York, 1995).
 - [2] T. Halpin-Healy and Y. C. Zhang, Phys. Rep.**245**,218(1995);J. Krug, Adv. Phys.**46**,139(1997)
 - [3] J. Krug and H. Spohn in "Solids Far from Equilibrium Growth, Morphology and Defects", edited by C. Godreche (Cambridge University Press, New York, 1990).
 - [4] P. Meakin, "Fractal, Scaling and Growth Far from Equilibrium" (Cambridge University Press, Cambridge,